

## Regular article

Functional characterization of 12 allelic variants of CYP2C8 by assessment of paclitaxel 6 $\alpha$ -hydroxylation and amodiaquine N-deethylationChiharu Tsukada<sup>a</sup>, Takahiro Saito<sup>a</sup>, Masamitsu Maekawa<sup>b</sup>, Nariyasu Mano<sup>b</sup>, Akifumi Oda<sup>c</sup>, Noriyasu Hirasawa<sup>a</sup>, Masahiro Hiratsuka<sup>a,\*</sup><sup>a</sup> Laboratory of Pharmacotherapy of Life-Style Related Diseases, Graduate School of Pharmaceutical Sciences, Tohoku University, Sendai 980-8578, Japan<sup>b</sup> Department of Pharmacy, Tohoku University Hospital, Sendai 980-8574, Japan<sup>c</sup> Institute of Medical, Pharmaceutical and Health Sciences, Kanazawa University, Kanazawa 920-1192, Japan

## ARTICLE INFO

## Article history:

Received 14 May 2015

Received in revised form

14 July 2015

Accepted 21 July 2015

Available online 31 July 2015

## Keywords:

Cytochrome P450

CYP2C8

Genetic polymorphisms

Paclitaxel

Amodiaquine

## ABSTRACT

Cytochrome P450 2C8 (CYP2C8) is one of the enzymes primarily responsible for the metabolism of many drugs, including paclitaxel and amodiaquine. CYP2C8 genetic variants contribute to interindividual variations in the therapeutic efficacy and toxicity of paclitaxel. Although it is difficult to investigate the enzymatic function of most CYP2C8 variants *in vivo*, this can be investigated *in vitro* using recombinant CYP2C8 protein variants. The present study used paclitaxel to evaluate 6 $\alpha$ -hydroxylase activity and amodiaquine for the N-deethylase activity of wild-type and 11 CYP2C8 variants resulting in amino acid substitutions *in vitro*. The wild-type and variant CYP2C8 proteins were heterologously expressed in COS-7 cells. Paclitaxel 6 $\alpha$ -hydroxylation and amodiaquine N-deethylation activities were determined by measuring the concentrations of 6 $\alpha$ -hydroxypaclitaxel and N-desethylamodiaquine, respectively, and the kinetic parameters were calculated. Compared to the wild-type enzyme (CYP2C8.1), CYP2C8.11 and CYP2C8.14 showed little or no activity with either substrate. In addition, the intrinsic clearance values of CYP2C8.8 and CYP2C8.13 for paclitaxel were 68% and 67% that of CYP2C8.1, respectively. In contrast, the  $CL_{int}$  values of CYP2C8.2 and CYP2C8.12 were 1.4 and 1.9 times higher than that of CYP2C8.1. These comprehensive findings could inform for further genotype-phenotype studies on interindividual differences in CYP2C8-mediated drug metabolism.

Copyright © 2015, The Japanese Society for the Study of Xenobiotics. Published by Elsevier Ltd. All rights reserved.

## 1. Introduction

Cytochrome P450 2C8 (CYP2C8) is a major metabolic enzyme that contributes to the metabolism of at least 5% of clinical drugs, including the anticancer drug, paclitaxel, and the antimalarial drug, amodiaquine [1]. Interindividual variability in cytochrome P450 activity significantly influences the metabolism of these drugs, resulting in alterations in efficacy and adverse effects. Recently, polymorphisms in CYP2C8 have been reported to contribute to alterations in enzymatic activity [2]. CYP2C8\*3 (2130G > A, 30411A > G; R139K, K399R), which is one of the major allelic variants of CYP2C8, has an allele frequency of 0.13 among Caucasians [3]. CYP2C8.3, the protein encoded by CYP2C8\*3, has been reported to show substrate-dependent alterations in activity [4–6].

Paclitaxel is useful for the treatment of breast, lung, and ovarian cancers. However, inter-patient variability in its toxicity (e.g., peripheral neuropathy and neutropenia) and therapeutic efficacy limit its use in chemotherapy [7–9]. Paclitaxel is primarily metabolized by CYP2C8, with secondary metabolism by CYP3A4/5 (Fig. 1). In a previous cohort study, Hertz et al. reported that breast cancer patients carrying the CYP2C8\*3 variant achieved a more complete clinical response to paclitaxel than did patients carrying the wild-type allele [10]. The odds ratio for an individual with the CYP2C8\*3 allele to achieve complete clinical response was 3.92. Subjects with CYP2C8\*3 were also more susceptible to severe peripheral neuropathy caused by paclitaxel, showing an odds ratio was 3.13. A study by Green et al. stratified thirty-eight ovarian cancer patients (treated with paclitaxel and carboplatin) by their ABCB1 G2677 T/A genotype, and found that those who were heterozygous for CYP2C8\*3 showed reduced clearance of paclitaxel [11]. Bergmann et al. reported that carriers of CYP2C8\*3 had 11% lower clearance than non-carriers [12]. In addition to CYP2C8\*3, a

\* Corresponding author.

E-mail address: [mhira@m.tohoku.ac.jp](mailto:mhira@m.tohoku.ac.jp) (M. Hiratsuka).

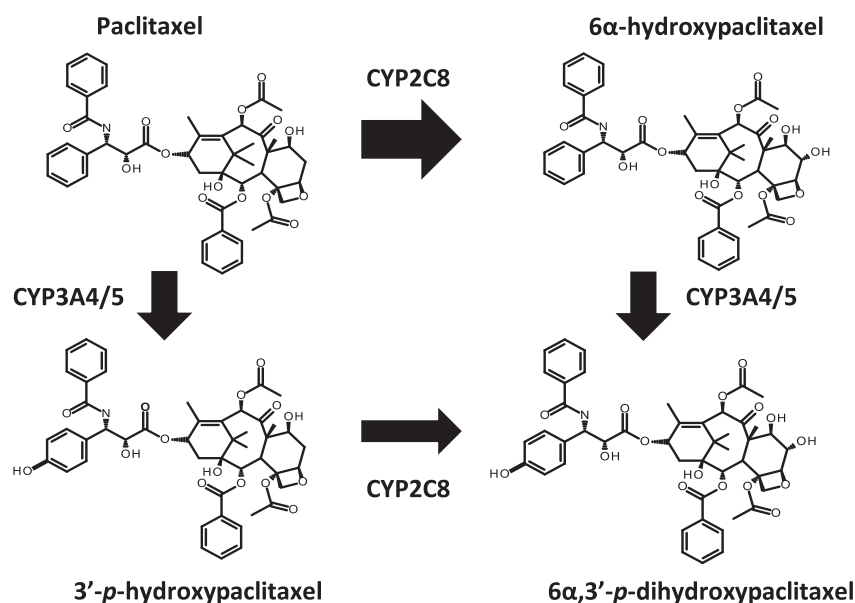


**Fig. 1.** Metabolic pathways for paclitaxel showing the primary route, catalyzed by cytochrome P450 2C8 (CYP2C8) and secondary routes, catalyzed by CYP3A4/5.

large study by Abraham et al. found that *CYP2C8\*4* was associated with an increased risk for paclitaxel-related peripheral neuropathy [13]. An association between *CYP2C8* genetic polymorphisms and changes in paclitaxel pharmacodynamics and pharmacokinetics has been found in several previous studies [14–16]. However, it is difficult to investigate the enzymatic function of most of the *CYP2C8* allelic variants *in vivo*. The association between these variants and patient responses to paclitaxel, or the incidence of severe adverse effects, is also difficult to determine because of their low frequency in the population (below 0.01) [17]. Therefore, most of their enzymatic functions *in vivo* remain unclear.

To assess the functional differences between the enzymatic activities of *CYP2C8* variants *in vitro*, previous studies have used a range of heterologous expression systems, including bacteria, yeast, insect cells, and mammalian cells [3,4,6,18–27]. Using these systems, several *CYP2C8* variants were shown to exhibit increased or decreased enzymatic activity for *CYP2C8* substrates. However, different kinetic values have been reported in the different expression systems used. Therefore, the present study expressed *CYP2C8* variants under the same conditions in mammalian cells and compared their catalytic activities.

To date, 16 variant alleles of *CYP2C8* have been designated (<http://www.cypalleles.ki.se/cyp2c8.htm>). A previous study showed that *CYP2C8\*5* and *CYP2C8\*7* variant alleles produced incomplete proteins that were not enzymatically active [24,28]. This lack of activity was due to a frame shift (for *CYP2C8\*5*) and a nonsense mutation (for *CYP2C8\*7*). In the present study, we focused on *CYP2C8\*1*–*CYP2C8\*14* (Table 1) and evaluated their function after their expression in COS-7 cells. The use of two *CYP2C8* substrates, paclitaxel and amodiaquine, enabled us to examine whether any functional differences were substrate-specific.

## 2. Materials and methods

### 2.1. Chemicals

Paclitaxel was purchased from Wako Pure Chemical Industries (Osaka, Japan). Docetaxel was purchased from Sigma–Aldrich (St Louis, MO, USA). 6 $\alpha$ -Hydroxypaclitaxel was obtained from Calbiochem (San Diego, CA, USA). Amodiaquine, *N*-desethylamodiaquine hydrochloride, and *N*-desethylamodiaquine-*d*<sub>5</sub> were purchased

from Toronto Research Chemicals (North York, Ontario, Canada). Oxidized  $\beta$ -nicotinamide-adenine dinucleotide phosphate (NADP<sup>+</sup>), glucose-6-phosphate (G6P), glucose-6-phosphate dehydrogenase (G6PDH), and  $\beta$ -nicotinamide-adenine dinucleotide phosphate (NADPH) were obtained from Oriental Yeast (Tokyo, Japan). The polyclonal anti-human *CYP2C8* antibody was purchased from Nosan Corporation (Kanagawa, Japan). The polyclonal anti-calnexin antibody was purchased from Enzo Life Sciences (Farmingdale, NY, USA). Polyclonal goat anti-rabbit immunoglobulin/horseradish peroxidase was purchased from DakoCytomation (Glostrup, Denmark). COS-7 cells were obtained from Riken Cell Bank (Ibaraki, Japan). All other chemicals and reagents were of the highest quality or analytical quality commercially available.

### 2.2. *CYP2C8* cDNA cloning and construction of expression vectors

*CYP2C8* cDNA fragments, obtained from a human liver cDNA library (TaKaRa, Shiga, Japan), were amplified by polymerase chain reaction with the forward primer 5'-CACCATGGAACCTTTTGTGGTCCTG-3' and the reverse primer 5'-TCAGACAGGGATGAAGCA-GATCTGGTATG-3' using PfuUltra High-Fidelity DNA polymerase (Agilent Technologies, Santa Clara, CA, USA). The underlined sequence in the forward primer was introduced for directional TOPO cloning. Amplified fragments were subcloned into the pENTR/D-TOPO vector (Life Technologies, Carlsbad, CA, USA). Plasmids containing *CYP2C8\*1* cDNA were used as a template to generate 11 *CYP2C8* allelic variant constructs (*CYP2C8\*2*–*CYP2C8\*4*, *CYP2C8\*6*, *CYP2C8\*8*–*CYP2C8\*14*) using a QuikChange Site-directed Mutagenesis Kit (Stratagene, La Jolla, CA, USA), according to the manufacturer's instructions. All prepared constructs were confirmed by direct sequencing. Wild type and variant *CYP2C8* cDNA sequences were subsequently subcloned into the mammalian expression vector, pcDNA3.4 (Life Technologies), by TA cloning.

### 2.3. Expression of *CYP2C8* variant proteins in COS-7 cells

COS-7 cells were cultured in Dulbecco's modified Eagle's medium (Nacalai Tesque, Kyoto, Japan) containing 10% fetal bovine serum at 37 °C in the presence of 5% CO<sub>2</sub>. Cells were transfected with plasmids (7  $\mu$ g) carrying *CYP2C8* cDNA using TransFectin lipid reagent (Bio-Rad Laboratories, Hercules, CA, USA), according to the

**Table 1**  
CYP2C8 allelic variants characterized in this study.

Allele	Protein	dbSNP number <sup>a</sup>	Nucleotide changes	Amino acid changes
CYP2C8*1	CYP2C8.1			
CYP2C8*2	CYP2C8.2	rs11572103	11054A > T	I269F
CYP2C8*3	CYP2C8.3	rs11572080; rs10509681	2130G > A; 30411A > G	R139K; K399R
CYP2C8*4	CYP2C8.4	rs1058930	11041C > G	I264M
CYP2C8*6	CYP2C8.6	rs142886225	4472G > A	G171S
CYP2C8*8	CYP2C8.8	rs72558195	4517C > T	R186G
CYP2C8*9	CYP2C8.9	–	10989A > G	K247R
CYP2C8*10	CYP2C8.10	–	26513G > T	K383N
CYP2C8*11	CYP2C8.11	rs78637576	23452G > T	E274X
CYP2C8*12	CYP2C8.12	rs3832694	32184_32186delTTG	461delV
CYP2C8*13	CYP2C8.13	–	10918T > G	I223M
CYP2C8*14	CYP2C8.14	rs188934928	10961G > C	A238P

CYP2C8, cytochrome P450 2C8; SNP, single nucleotide polymorphism.

<sup>a</sup> RefSNP accession number in dbSNP (<http://www.ncbi.nlm.nih.gov/snp/>).

manufacturer's instructions. After incubation for 24 h at 37 °C, cells were scraped off, centrifuged at 1500 g for 5 min, and re-suspended in homogenization buffer (10 mM Tris–HCl [pH 7.4], 1 mM ethylenediaminetetraacetic acid [EDTA], and 10% glycerol). Microsomal fractions were prepared by differential centrifugation at 9000 g for 20 min, followed by centrifugation of the resulting supernatant at 105 000 g for 60 min. The microsomal pellet was re-suspended in 50 mM Tris–HCl (pH 7.4) containing 1 mM EDTA, 20% glycerol, 150 mM KCl, and Protease Inhibitor Cocktail Set III (Calbiochem) and stored at –80 °C. The protein concentration was determined using a BCA protein assay kit (Thermo Fisher Scientific, Waltham, MA, USA).

#### 2.4. Determination of protein expression levels by immunoblotting

COS-7 microsomal fractions (2 µg microsomal protein) were separated by electrophoresis on 10% sodium dodecyl sulfate-polyacrylamide gels. Western blotting was performed according to standard procedures. Recombinant CYP2C8 Supersomes (BD Biosciences, Woburn, MA, USA) were used as the standard (range, 0.02–0.25 pmol) in each gel to quantify the CYP2C8 protein level. CYP2C8 protein was detected using a polyclonal anti-human CYP2C8 antibody (diluted at 1:1000), and calnexin was detected by a polyclonal anti-calnexin antibody (diluted at 1:5000). Secondary detection was carried out with horseradish peroxidase-conjugated goat anti-rabbit IgG (diluted at 1:10 000). Immunoblots were visualized using SuperSignal West Femto Maximum Sensitivity Substrate (Thermo Fisher Scientific). Chemiluminescence was quantified using a ChemiDoc XRS<sup>+</sup>, with the help of Image Lab Software (Bio-Rad Laboratories).

#### 2.5. Paclitaxel 6 $\alpha$ -hydroxylation assay

Paclitaxel 6 $\alpha$ -hydroxylation by CYP2C8 was measured as reported previously, with several modifications [18]. The incubation mixture consisted of the microsomal fraction (50 µg), paclitaxel (0.25, 0.5, 1.0, 2.5, 5.0, 10, 20, 40, or 80 µM), and 50 mM potassium phosphate buffer (pH 7.4) in a total volume of 150 µL. Following pre-incubation at 37 °C for 3 min, reactions were initiated by addition of the NADPH-generating system (1.3 mM NADP<sup>+</sup>, 3.3 mM G6P, 3.3 mM magnesium chloride, and 0.4 units/mL G6PDH). The mixture was incubated at 37 °C for 20 min. Reactions were terminated by adding 150 µL of methanol containing 2 µM docetaxel (the internal standard). Measurement of paclitaxel 6 $\alpha$ -hydroxylation using 40 µM paclitaxel and 50 µg of the microsomal fraction containing CYP2C8.1 showed that 6 $\alpha$ -hydroxypaclitaxel formation was linear for incubations of up to 20 min. Moreover, when the reaction containing 40 µM paclitaxel was incubated for

20 min, 6 $\alpha$ -hydroxypaclitaxel formation was linear in the presence of up to 50 µg microsomal protein (data not shown).

After protein removal by centrifugation (10 000 × g for 3 min), 50 µL of the supernatant was subjected to high-performance liquid chromatography (HPLC). The HPLC system consisted of a Waters 2695 Separations Module, a Waters 2487 dual  $\lambda$  absorbance detector (Waters, Milford, MA, USA), and an XBridge C18 analytical column (4.6 × 150 mm, 5 µm particle size; Waters), maintained at 40 °C. 6 $\alpha$ -Hydroxypaclitaxel was eluted isocratically with water and acetonitrile (60:40, v/v) at a flow rate of 1.0 mL/min. Detection of 6 $\alpha$ -hydroxypaclitaxel was performed by measuring absorbance at 230 nm. The lower limit of 6 $\alpha$ -hydroxypaclitaxel quantification was 10 nM. Standard curves for 6 $\alpha$ -hydroxypaclitaxel were constructed in the 0.01–4 µM range using authentic metabolite. The coefficient of variation was 6.3% for a 6 $\alpha$ -hydroxypaclitaxel concentration of 0.8 µM, which was observed at substrate concentrations in the range of Michaelis constant ( $K_m$ ). The enzymatic activity was normalized to the CYP2C8 expression level.

#### 2.6. Amodiaquine N-deethylation assay

The amodiaquine N-deethylation activity of CYP2C8 was determined using previously reported methods, with minor modifications [29]. The reaction mixture contained the microsomal fraction (15 µg), amodiaquine (0.25, 0.5, 1.0, 2.5, 5.0, 10, 20, 40, or 80 µM), and 50 mM potassium phosphate buffer (pH 7.4) in a total volume of 150 µL. Following pre-incubation at 37 °C for 3 min, reactions were initiated by the addition of 1 mM NADPH. The mixtures were incubated for an additional 20 min at 37 °C. Reactions were terminated by adding 150 µL acetonitrile containing 300 nM N-desethylamodiaquine-d<sub>5</sub> (the internal standard). Determination of amodiaquine N-deethylation activity in the microsomal fraction containing CYP2C8.1 (20 µg of microsomal protein) and 40 µM amodiaquine revealed that N-desethylamodiaquine formation was linear for incubations of up to 20 min. When the reaction containing 40 µM amodiaquine was incubated for 20 min, N-desethylamodiaquine formation was linear in the presence of up to 15 µg of microsomal protein (data not shown).

After the removal of protein by centrifugation (15 000 × g for 10 min), the supernatant was diluted five times with water, and 10 µL of the diluted solution was injected into a liquid chromatography tandem mass spectrometry (LC-MS/MS) system. N-Desethylamodiaquine was measured using the LC-MS/MS system in the positive ion detection mode at the electrospray ionization interface (TSQ Vantage Triple Stage Quadrupole Mass Spectrometer; Thermo Fisher Scientific). Separation by ultra HPLC was conducted using a Nexera Ultra High Performance Liquid Chromatography system (SHIMADZU, Kyoto, Japan). Chromatographic separation was

performed using an XBridge C18 analytical column (2.1 × 150 mm, 3.5 μm particle size; Waters), maintained at 50 °C. *N*-Desethylamodiaquine was eluted isocratically with a mobile phase consisting of 5 mM ammonium acetate and 0.1% (v/v) formic acid in water and 5 mM ammonium acetate and 0.1% (v/v) formic acid in acetonitrile (90:10, v/v) at a flow rate of 200 μL/min.

Quantitative MS/MS analyses were performed in the selective reaction monitoring mode. The areas under the peak of the *m/z* 328 → 283 (collision energy, 17 V and S-Lens RF amplitude voltage, 67 V) for *N*-desethylamodiaquine and that of the *m/z* 333 → 283 (collision energy, 15 V and S-Lens RF amplitude voltage, 66 V) for *N*-desethylamodiaquine-*d*<sub>5</sub> were measured. The optimized parameters for MS were as follows: spray voltage, 3.5 kV; sheath gas pressure, 50 psi; vaporizer temperature, 400 °C; capillary temperature, 392 °C; and collision pressure, 1.4 mTorr. The sheath gas was nitrogen, and the collision gas was argon. The LC-MS/MS system was controlled by Xcalibur software (Thermo Fisher Scientific), which was also used to analyze the data. The lower limit of *N*-desethylamodiaquine quantification was 5 nM. Standard curves for *N*-desethylamodiaquine were constructed in the 5–2560 nM range using authentic metabolite. The coefficient of variation was 2.4% for an *N*-desethylamodiaquine concentration of 160 nM, which was observed at substrate concentrations in the range of *K<sub>m</sub>*. The enzymatic activity was normalized to the corresponding CYP2C8 expression level.

### 2.7. Data analysis

The kinetic data were analyzed in the Enzyme Kinetics Module of SigmaPlot 12.0 (Systat Software, Inc., Chicago, IL, USA), a curve-fitting program based on nonlinear regression analysis, and the *K<sub>m</sub>*, maximum velocity (*V<sub>max</sub>*), and intrinsic clearance (*CL<sub>int</sub>* = *V<sub>max</sub>*/*K<sub>m</sub>*) values were determined. All values were expressed as the mean ± standard deviation (SD) of experiments performed in triplicate. Statistical analyses of enzymatic activity and kinetic parameters used analysis of variance, Dunnett's test for *CL<sub>int</sub>* of paclitaxel, and Dunnett's T3 test for the paclitaxel *K<sub>m</sub>* and *V<sub>max</sub>* and for the amodiaquine *CL<sub>int</sub>*, *K<sub>m</sub>*, and *V<sub>max</sub>* (IBM SPSS Statistics, International Business Machines, Armonk, NY, USA). Differences with *P*-values less than 0.05 were considered statistically significant.

### 2.8. 3D structural modeling of CYP2C8

CYP2C8 3D structural modeling was based on the CYP2C8 X-ray structure reported by Schoch et al., Protein Data Bank code: 1PQ2 [30]. The CDocker protocol of Discovery Studio 2.5 (Accelrys, San Diego, CA, USA) was used to create docked CYP2C8-paclitaxel and CYP2C8-amodiaquine structures.

## 3. Results

Protein levels of the CYP2C8 variants expressed in COS-7 cells were measured by immunoblotting. The polyclonal CYP2C8 antibodies recognized all CYP2C8 variant proteins (Fig. 2). Expression levels of the endoplasmic reticulum-resident protein, calnexin, were almost constant in microsomes from the transfected cells. CYP2C8 protein was not detected in the cells transfected with empty vector (mock transfection).

The kinetic parameters of paclitaxel 6α-hydroxylation were determined for 10 CYP2C8 variants, as shown in Table 2. For CYP2C8.11, 6α-hydroxypaclitaxel was not detected, even at the highest concentration of paclitaxel tested (80 μM). *K<sub>m</sub>*, *V<sub>max</sub>*, and *CL<sub>int</sub>* values for paclitaxel 6α-hydroxylation by the wild-type enzyme (CYP2C8.1) were 7.18 μM, 2.18 pmol min<sup>-1</sup> pmol<sup>-1</sup> CYP2C8, and 0.31 μL min<sup>-1</sup> pmol<sup>-1</sup> CYP2C8, respectively. The *K<sub>m</sub>*

value for CYP2C8.8 was reduced to 25% of that for wild-type. Compared to the *V<sub>max</sub>* value for CYP2C8.1, the *V<sub>max</sub>* values for CYP2C8.9 and CYP2C8.12 were significantly increased (by 1.2- and 1.3-fold, respectively). The *V<sub>max</sub>* values of CYP2C8.3, CYP2C8.4, CYP2C8.8, CYP2C8.10, CYP2C8.13, and CYP2C8.14 were significantly decreased. The *CL<sub>int</sub>* values for CYP2C8.2 and CYP2C8.12 were significantly higher, and those of CYP2C8.3, CYP2C8.8, CYP2C8.13, and CYP2C8.14 were significantly lower than that of CYP2C8.1.

The kinetics of amodiaquine *N*-deethylation were determined for nine CYP2C8 variants, as shown in Table 3. The *K<sub>m</sub>*, *V<sub>max</sub>*, and *CL<sub>int</sub>* for amodiaquine *N*-deethylation by CYP2C8.1 were 1.35 μM, 11.3 pmol min<sup>-1</sup> pmol<sup>-1</sup> CYP2C8, and 8.37 μL min<sup>-1</sup> pmol<sup>-1</sup> CYP2C8, respectively. The kinetic parameters of CYP2C8.11 and CYP2C8.14 could not be determined because the amount of the product, *N*-desethylamodiaquine, produced by these variants was below the limit of quantification at low substrate concentrations. Three variants, CYP2C8.2, CYP2C8.4, and CYP2C8.6, showed *K<sub>m</sub>* values that were 1.3-fold higher than that of CYP2C8.1. The *V<sub>max</sub>* for CYP2C8.2 was also increased 1.4-fold over that of CYP2C8.1. The *V<sub>max</sub>* values of CYP2C8.3, CYP2C8.6, CYP2C8.8, CYP2C8.9, CYP2C8.10, CYP2C8.12, and CYP2C8.13 were significantly lower than that of CYP2C8.1. The *CL<sub>int</sub>* values of six variants, CYP2C8.6, CYP2C8.8, CYP2C8.9, CYP2C8.10, CYP2C8.12, and CYP2C8.13, were significantly lower than the *CL<sub>int</sub>* for CYP2C8.1.

## 4. Discussion

CYP2C8 is a clinically important metabolic enzyme. It has been recognized that CYP2C8 genetic polymorphisms are a possible source of interindividual variability in the efficacy and adverse effects of drugs metabolized by this enzyme. The present study revealed, for the first time, functional alterations in the activities of 11 CYP2C8 allelic variants expressed in COS-7 cells. The kinetic parameters for paclitaxel 6α-hydroxylation were determined for 10 variants and those for amodiaquine *N*-deethylation were determined for 9 variants. The kinetics of wild-type and variant forms of CYP2C8 determined in this study and in other studies are shown in Supplemental Table 1.

Some studies have reported that CYP2C8.4, which includes an I264M substitution, showed altered enzymatic activity (Supplemental Table 1). Although previous *in vitro* studies reported reduced paclitaxel clearance by CYP2C8.4, as compared with the wild-type enzyme, our study did not identify any statistically significant difference in *CL<sub>int</sub>*. This inconsistency may reflect the different experimental systems employed (Supplemental Table 1). It has been reported that the I264M substitution in CYP2C8.4 decreased the ratio of holoprotein to apoprotein and made CYP2C8.4 less thermally stable than CYP2C8.1 [22]. Moreover,

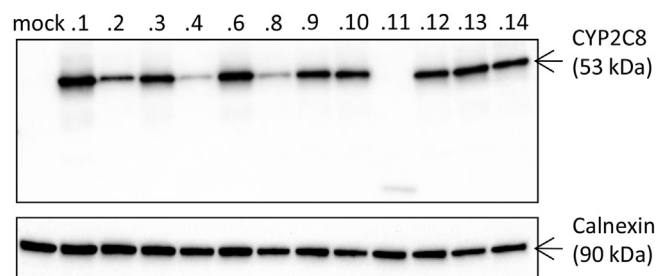


**Fig. 2.** Western blots showing immunoreactive cytochrome P450 2C8 (CYP2C8) variant proteins (upper panel) and calnexin (lower panel). Following electrophoresis on 10% sodium dodecyl sulfate-polyacrylamide gels and protein transfer, CYP2C8 variant proteins and calnexin (loading control) were detected using polyclonal antibodies. The lane numbers in the upper panel correspond to the CYP2C8 variant expressed in the sample (see Table 1).

**Table 2**  
Kinetic parameters for paclitaxel 6 $\alpha$ -hydroxylation by microsomes of COS-7 cells expressing wild-type (CYP2C8.1) and CYP2C8 allelic variants.

Variant	$K_m$ ( $\mu\text{M}$ )	$V_{max}$ ( $\text{pmol min}^{-1} \text{pmol}^{-1}$ CYP2C8)	$CL_{int}$ ( $\mu\text{L min}^{-1} \text{pmol}^{-1}$ CYP2C8) (% of CYP2C8.1)
CYP2C8.1	7.18 $\pm$ 0.62	2.18 $\pm$ 0.06	0.30 $\pm$ 0.02
CYP2C8.2	8.37 $\pm$ 1.87	3.60 $\pm$ 0.41	0.44 $\pm$ 0.05*** (143%)
CYP2C8.3	6.02 $\pm$ 0.53	1.25 $\pm$ 0.02***	0.21 $\pm$ 0.02*** (68%)
CYP2C8.4	5.15 $\pm$ 0.85	1.26 $\pm$ 0.04***	0.25 $\pm$ 0.03 (81%)
CYP2C8.6	6.54 $\pm$ 0.55	1.86 $\pm$ 0.07	0.29 $\pm$ 0.014 (94%)
CYP2C8.8	1.78 $\pm$ 0.40**	0.34 $\pm$ 0.02***	0.20 $\pm$ 0.03*** (65%)
CYP2C8.9	6.90 $\pm$ 0.30	2.59 $\pm$ 0.03*	0.38 $\pm$ 0.01* (123%)
CYP2C8.10	5.05 $\pm$ 0.27	1.40 $\pm$ 0.02***	0.28 $\pm$ 0.003 (91%)
CYP2C8.12	4.88 $\pm$ 0.46	2.85 $\pm$ 0.13**	0.59 $\pm$ 0.04* (192%)
CYP2C8.13	5.25 $\pm$ 0.93	1.06 $\pm$ 0.08***	0.20 $\pm$ 0.02*** (67%)
CYP2C8.14	17.7 $\pm$ 3.15***	0.71 $\pm$ 0.09***	0.04 $\pm$ 0.002*** (13%)

CYP2C8, cytochrome P450 2C8;  $K_m$ , Michaelis constant;  $V_{max}$ , maximum velocity;  $CL_{int}$ , intrinsic clearance ( $V_{max}/K_m$ ). These data represent the mean  $\pm$  SD of three independent catalytic assays. \* $P < 0.05$ , \*\* $P < 0.01$ , \*\*\* $P < 0.005$ , as compared to CYP2C8.1. The kinetics of CYP2C8.11 could not be determined because its enzymatic activity was not detected at a high substrate concentration (80  $\mu\text{M}$  paclitaxel).

**Table 3**  
Kinetic parameters for amodiaquine N-deethylation by microsomes of COS-7 cells expressing wild-type (CYP2C8.1) and CYP2C8 allelic variants.

Variants	$K_m$ ( $\mu\text{M}$ )	$V_{max}$ ( $\text{pmol min}^{-1} \text{pmol}^{-1}$ CYP2C8)	$CL_{int}$ ( $\mu\text{L min}^{-1} \text{pmol}^{-1}$ CYP2C8) (% of CYP2C8.1)
CYP2C8.1	1.35 $\pm$ 0.036	11.30 $\pm$ 0.15	8.37 $\pm$ 0.29
CYP2C8.2	1.76 $\pm$ 0.037***	16.13 $\pm$ 0.23***	9.18 $\pm$ 0.07 (110%)
CYP2C8.3	1.19 $\pm$ 0.095	8.41 $\pm$ 0.11***	7.11 $\pm$ 0.48 (85%)
CYP2C8.4	1.70 $\pm$ 0.022***	11.28 $\pm$ 0.13	6.62 $\pm$ 0.03 (79%)
CYP2C8.6	1.78 $\pm$ 0.053**	5.81 $\pm$ 0.03***	3.26 $\pm$ 0.09*** (39%)
CYP2C8.8	1.31 $\pm$ 0.062	3.45 $\pm$ 0.10***	2.65 $\pm$ 0.05*** (32%)
CYP2C8.9	1.28 $\pm$ 0.092	5.49 $\pm$ 0.09***	4.31 $\pm$ 0.25*** (52%)
CYP2C8.10	1.18 $\pm$ 0.063*	3.88 $\pm$ 0.04***	3.29 $\pm$ 0.15*** (39%)
CYP2C8.12	1.13 $\pm$ 0.093***	4.40 $\pm$ 0.17***	3.92 $\pm$ 0.49** (47%)
CYP2C8.13	1.48 $\pm$ 0.032	2.69 $\pm$ 0.01***	1.82 $\pm$ 0.04*** (22%)

CYP2C8, cytochrome P450 2C8;  $K_m$ , Michaelis constant;  $V_{max}$ , maximum velocity;  $CL_{int}$ , intrinsic clearance ( $V_{max}/K_m$ ). These data represent the mean  $\pm$  SD of three independent catalytic assays. \* $P < 0.05$ , \*\* $P < 0.01$ , \*\*\* $P < 0.005$ , as compared to CYP2C8.1. The kinetic parameters of CYP2C8.11 and CYP2C8.14 could not be determined because the amount of metabolite produced was below the detection limit at the lower substrate concentrations.

CYP2C8.4 has been shown to be more susceptible to proteasomal degradation than the wild-type enzyme, resulting in decreased protein levels and correspondingly lower enzyme activity [23]. CYP2C8.4 may therefore be less stable than CYP2C8.1 and further investigation of its stability and expression level is required.

The CYP2C8\*2 allele contains the nucleotide change 11054A > T, which produces the I269F substitution. This is one of the most common variants of CYP2C8. Previous studies using other expression systems reported that the recombinant CYP2C8.2 enzyme had lower  $CL_{int}$  values for paclitaxel and amodiaquine metabolism, as compared with CYP2C8.1 [3,4,18,19]. However, the data presented in this study indicated that CYP2C8.2 showed a significantly higher  $CL_{int}$  for paclitaxel than did CYP2C8.1. Inconsistencies between the present and previous studies in terms of paclitaxel metabolism in transient expression systems may be due to differences in the experimental systems employed (*Escherichia coli*, yeast, and insect cells). Additionally, the I269F substitution is located in the H-helix on the surface of the CYP2C8 protein; this is close to the I264M substitution found in CYP2C8.4. Thus, CYP2C8.2 may also be less stable, resulting in decreased activity *in vivo*; however, *in vitro*, CYP2C8.2 activity was increased. Further investigation is needed to determine how the I269F substitution in CYP2C8.2 affects the pharmacokinetics of CYP2C8 substrates *in vivo*. Aquilante et al. reported that the mean area under the concentration-time (0–48 h) curve ( $AUC_{0-48}$ ) of the ratio of two pioglitazone metabolites (M-III:M-IV) was 33% lower in CYP2C8\*2 carriers than in wild-type carriers; however, the maximum plasma concentration and AUC of pioglitazone did not differ significantly between these individuals [31]. Hertz et al. reported an association between the CYP2C8 genotype and paclitaxel-induced peripheral neuropathy (PIPNe) [16]. In this study, CYP2C8\*2, CYP2C8\*3, and CYP2C8\*4 carriers were categorized as low paclitaxel metabolizers, but neither

CYP2C8\*2 nor CYP2C8\*4 carriage showed a significant association with PIPNe. In the present study, the data indicated that CYP2C8\*2 may not reduce drug metabolism. Therefore, the impact of CYP2C8\*2 on the pharmacokinetics of drugs metabolized by CYP2C8 remains unclear. Further studies will be required to determine the impact of this genotype on drug metabolism in clinical settings.

CYP2C8.8, which contains an R186G substitution, showed a lower level of expressed protein than did CYP2C8.1 and substantially decreased activities for both substrates; this was consistent with the results of a previous study [24]. Additionally, it has been reported that the CYP2C8.8 holoprotein level expressed in insect cells was significantly lower than that of CYP2C8.1 [24]. R186 in CYP2C8.1 is located in the E-F loop, forming an ionic bond with E148 in the D-helix. The R186G substitution in CYP2C8.8 may cause a loss of this ionic bonding and may lead to hydrogen bonding with E147 instead (Fig. 3). This conformational alteration may reduce the affinity for heme and alter the ratio of holoprotein forms, making CYP2C8.8 more susceptible to proteasomal degradation.

CYP2C8\*11 contains the nucleotide change 23452G > T, which produces the E274X substitution. Consequently, CYP2C8.11 lacks approximately 40% of the C-terminal region, including the heme binding site. The present study found that CYP2C8.11 was inactive for both substrates. Yeo et al. reported that the CYP2C8\*11 genotype caused a decrease in rosiglitazone hydroxylation *in vivo* [32]. Subjects with CYP2C8\*1/\*11 heterozygosity showed a 31% decrease in rosiglitazone hydroxylation, as compared with CYP2C8\*1 homozygotes. These findings indicated that patients with CYP2C8\*11 would show decreased paclitaxel 6 $\alpha$ -hydroxylation, resulting in more severe adverse effects, including peripheral neuropathy and neutropenia.

The present study revealed previously uncharacterized functional alterations in CYP2C8.12 activity. This variant showed a markedly increased  $V_{max}$  for paclitaxel and a significantly decreased

$V_{max}$  for amodiaquine, as compared to the wild-type enzyme. Thus, CYP2C8.12 exhibited substrate specificity in its activity. The deletion of three nucleotides, TTG, at residues 32184–32186 in CYP2C8\*12, results in the deletion of V461 (461delV). This allele is found at a very low frequency in the Japanese population (0.1%) [17]. V461 is located in the C-terminal region of CYP2C8.1. The next residue, D462, may form a hydrogen bond with N466. In CYP2C8.12, 461delV caused a shift to D461, which may form a hydrogen bond with N465. Furthermore, D462 may also form a hydrogen bond with N465 (Fig. 4A). Thereby, conformational changes in the active sites, including the important residue I476, which is I475 in CYP2C8.12, may occur (Fig. 4B). The differential activities for

paclitaxel and amodiaquine may relate to structural and size differences between paclitaxel (molecular weight, 854) and amodiaquine (molecular weight, 356), and to the size of the active sites.

The  $V_{max}$  of CYP2C8.13 was significantly decreased for both substrates. This variant contains the I223M substitution in the F'-helix. The M side chain is bulkier than that of I and the I223M substitution may therefore result in steric hindrance and improper protein folding. Afzelius et al. reported that the conformational flexibility in the F-G loop in CYP2C5 and CYP2C9 could be of great importance for substrate recognition, binding, and the volume of the active site [33]. Therefore, CYP2C8.13 may reduce the flexibility of the F-G loop, resulting in decreased  $V_{max}$  and  $CL_{int}$ .

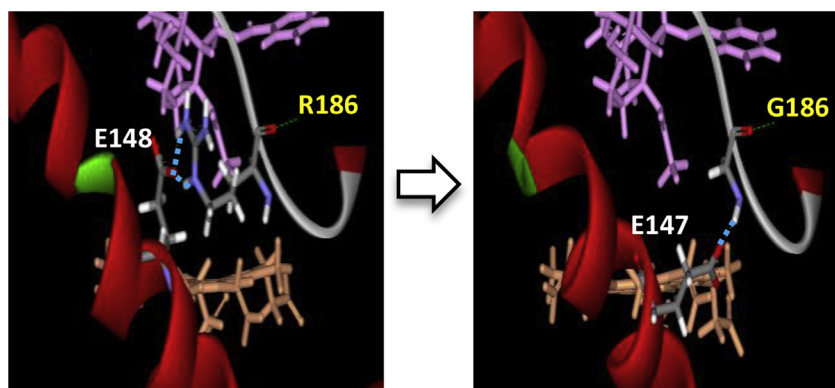


**Fig. 3.** A diagram of a portion of the crystal structure of cytochrome P450 2C8 (CYP2C8) showing the R186G substitution in CYP2C8.8. Paclitaxel is shown in pink, heme is shown in orange. Ionic bonding differs between the wild-type enzyme and the CYP2C8.8 variant.

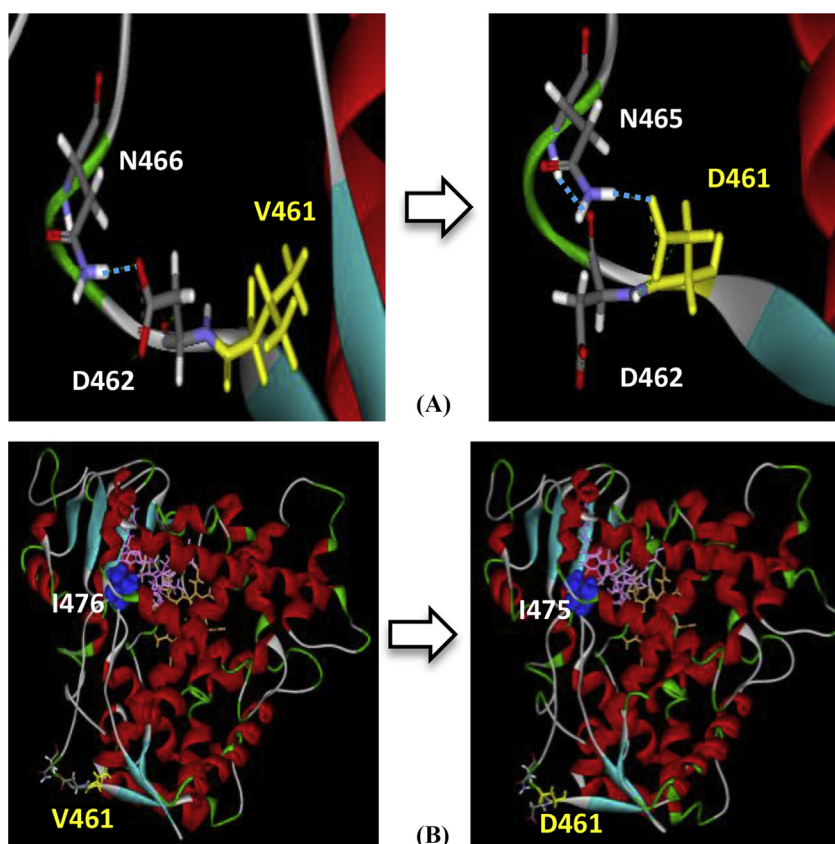


**Fig. 4.** (A) A diagram of a portion of the crystal structure of cytochrome P450 2C8 (CYP2C8), showing V461 and D461 (caused by the V deletion). V461 in the wild-type enzyme and D461 in CYP2C8.12 are shown in yellow. Hydrogen bonding differs between the wild-type enzyme and the CYP2C8.12 variant. (B) A diagram of the overall crystal structure of CYP2C8. Paclitaxel is shown in pink, heme is shown in orange, and the I476 residue in the wild-type enzyme and I475 residue in CYP2C8.12 are shown in blue. The size of the active site differs between the wild-type enzyme and the CYP2C8.12 variant.

CYP2C8.14 showed markedly decreased activity for both substrates. CYP2C8.14 has an A238P substitution in the G-helix. The residue A238 is located in the substrate recognition site, which is involved in substrate affinity [34]. Moreover, Hanioka et al. [26] reported that yeast expression of CYP2C8.14 produced a significantly lower holoprotein level than that observed for the wild-type enzyme, CYP2C8.1. Therefore, the CYP2C8.14 holoprotein levels may be decreased in comparison to those of CYP2C8.1, resulting in reduced metabolism of CYP2C8 substrates.

A study by Bergmann et al. found that CYP2C8\*3 carriers had a significantly lower clearance of paclitaxel than non-carriers, which was consistent with our *in vitro* data for CYP2C8\*3. However, there are some limitations to predicting *in vivo* activity or phenotype from *in vitro* data. Expression levels and protein stability may be considerably different *in vivo*. Some CYP2C8 variant proteins may decrease heme incorporation into the CYP2C8 apoprotein, but this possibility could not be assessed in the present study because we used polyclonal anti-human CYP2C8 antibodies to determine CYP2C8 protein levels. This could be investigated by studying the difference in the carbon monoxide-reduced spectra and by analyzing the protein bands using MS. Ohtsuki et al. have developed such an approach to the quantification of various CYP proteins [35]. These quantitative analyses would also overcome the potential limitation of antibody affinity differences between the variant proteins, and could determine the active form of CYP2C8 protein. However, the levels of CYP2C8 protein expressed in COS-7 cells were too low to analyze by the carbon monoxide-reduced spectra. Furthermore, the relationship between *in vivo* and *in vitro* data using other substrates are required to confirm these results, in addition to the measurement of the holoprotein level. Therefore, further studies will be required to determine the impact of these CYP2C8 allelic variants on drug metabolism in clinical settings.

In conclusion, wild-type CYP2C8 and 11 allelic variants of this enzyme were expressed in COS-7 cells and their enzymatic activities were characterized *in vitro*. This study confirmed the functional alterations previously reported for some variants and also characterized the activity of several other less common allelic variants. These variants could contribute to significant interindividual variability in the pharmacokinetics and pharmacodynamics of drugs that are CYP2C8 substrates, such as paclitaxel and amodiaquine. These comprehensive findings may provide useful information for further genotype-phenotype correlation studies regarding interindividual differences in drug efficacy and toxicity arising from differences in CYP2C8 activity.

## Acknowledgments

This study was supported in part by a grant from the Ministry of Health, Labour and Welfare (MHLW) of Japan ('Initiative to facilitate development of innovative drug, medical devices, and cellular & tissue-based product'), the Smoking Research Foundation, and the Japan Research Foundation for Clinical Pharmacology. We thank the Biomedical Research Core of Tohoku University Graduate School of Medicine for technical support.

## Appendix A. Supplementary data

Supplementary data related to this article can be found at <http://dx.doi.org/10.1016/j.dmpk.2015.07.003>.

## References

- [1] Lai XS, Yang LP, Li XT, Liu JP, Zhou ZW, Zhou SF. Human CYP2C8: structure, substrate specificity, inhibitor selectivity, inducers and polymorphisms. *Curr Drug Metab* 2009;10:1009–47.
- [2] Aquilante CL, Niemi M, Gong L, Altman RB, Klein TE. PharmGKB summary: very important pharmacogene information for cytochrome P450, family 2, subfamily C, polypeptide 8. *Pharmacogenet Genomics* 2013;23:721–8.
- [3] Dai D, Zeldin DC, Blaisdell JA, Chanas B, Coulter SJ, Ghanayem BI, et al. Polymorphisms in human CYP2C8 decrease metabolism of the anticancer drug paclitaxel and arachidonic acid. *Pharmacogenetics* 2001;11:597–607.
- [4] Yu L, Shi D, Ma L, Zhou Q, Zeng S. Influence of CYP2C8 polymorphisms on the hydroxylation metabolism of paclitaxel, repaglinide and ibuprofen enantiomers *in vitro*. *Biopharm Drug Dispos* 2013;34:278–87.
- [5] Kaspera R, Narahariseti SB, Evangelista EA, Marcianite KD, Psaty BM, Totah RA. Drug metabolism by CYP2C8.3 is determined by substrate dependent interactions with cytochrome P450 reductase and cytochrome b5. *Biochem Pharmacol* 2011;82:681–91.
- [6] Kaspera R, Narahariseti SB, Tamraz B, Sahele T, Cheesman MJ, Kwok PY, et al. Cerivastatin *in vitro* metabolism by CYP2C8 variants found in patients experiencing rhabdomyolysis. *Pharmacogenet Genomics* 2010;20:619–29.
- [7] Steed H, Sawyer MB. Pharmacology, pharmacokinetics and pharmacogenomics of paclitaxel. *Pharmacogenomics* 2007;8:803–15.
- [8] Taniguchi R, Kumai T, Matsumoto N, Watanabe M, Kamio K, Suzuki S, et al. Utilization of human liver microsomes to explain individual differences in paclitaxel metabolism by CYP2C8 and CYP3A4. *J Pharmacol Sci* 2005;97:83–90.
- [9] Sonnichsen DS, Liu Q, Schuetz EG, Schuetz JD, Pappo A, Relling MV. Variability in human cytochrome P450 paclitaxel metabolism. *J Pharmacol Exp Ther* 1995;275:566–75.
- [10] Hertz DL, Motsinger-Reif AA, Drobish A, Winham SJ, McLeod HL, Carey LA, et al. CYP2C8\*3 predicts benefit/risk profile in breast cancer patients receiving neoadjuvant paclitaxel. *Breast Cancer Res Treat* 2012;134:401–10.
- [11] Green H, Soderkvist P, Rosenberg P, Mirghani RA, Rymark P, Lundqvist EA, et al. Pharmacogenetic studies of Paclitaxel in the treatment of ovarian cancer. *Basic Clin Pharmacol Toxicol* 2009;104:130–7.
- [12] Bergmann TK, Brasch-Andersen C, Green H, Mirza M, Pedersen RS, Nielsen F, et al. Impact of CYP2C8\*3 on paclitaxel clearance: a population pharmacokinetic and pharmacogenomic study in 93 patients with ovarian cancer. *Pharmacogenomics J* 2011;11:113–20.
- [13] Abraham JE, Guo Q, Dorling L, Tyrer J, Ingle S, Hardy R, et al. Replication of genetic polymorphisms reported to be associated with Taxane-related sensory neuropathy in early breast cancer patients treated with paclitaxel. *Clin Cancer Res* 2014;20:2466–75.
- [14] Leskela S, Jara C, Leandro-Garcia LJ, Martinez A, Garcia-Donas J, Hernando S, et al. Polymorphisms in cytochromes P450 2C8 and 3A5 are associated with paclitaxel neurotoxicity. *Pharmacogenomics J* 2011;11:121–9.
- [15] Green H, Khan MS, Jakobsen-Falk I, Avall-Lundqvist E, Peterson C. Impact of CYP3A5\*3 and CYP2C8-HapC on paclitaxel/carboplatin-induced myelosuppression in patients with ovarian cancer. *J Pharm Sci* 2011;100:4205–9.
- [16] Hertz DL, Roy S, Jack J, Motsinger-Reif AA, Drobish A, Clark LS, et al. Genetic heterogeneity beyond CYP2C8\*3 does not explain differential sensitivity to paclitaxel-induced neuropathy. *Breast Cancer Res Treat* 2014;145:245–54.
- [17] Saito Y, Katori N, Soyama A, Nakajima Y, Yoshitani T, Kim SR, et al. CYP2C8 haplotype structures and their influence on pharmacokinetics of paclitaxel in a Japanese population. *Pharmacogenet Genomics* 2007;17:461–71.
- [18] Gao Y, Liu D, Wang H, Zhu J, Chen C. Functional characterization of five CYP2C8 variants and prediction of CYP2C8 genotype-dependent effects on *in vitro* and *in vivo* drug-drug interactions. *Xenobiotica* 2010;40:467–75.
- [19] Parikh S, Ouedraogo JB, Goldstein JA, Rosenthal PJ, Kroetz DL. Amodiaquine metabolism is impaired by common polymorphisms in CYP2C8: implications for malaria treatment in Africa. *Clin Pharmacol Ther* 2007;82:197–203.
- [20] Soyama A, Saito Y, Hanioka N, Murayama N, Nakajima O, Katori N, et al. Non-synonymous single nucleotide alterations found in the CYP2C8 gene result in reduced *in vitro* paclitaxel metabolism. *Biol Pharm Bull* 2001;24:1427–30.
- [21] Soyama A, Saito Y, Komamura K, Ueno K, Kamakura S, Ozawa S, et al. Five novel single nucleotide polymorphisms in the CYP2C8 gene, one of which induces a frame-shift. *Drug Metab Pharmacokinet* 2002;17:374–7.
- [22] Jiang H, Zhong F, Sun L, Feng W, Huang ZX, Tan X. Structural and functional insights into polymorphic enzymes of cytochrome P450 2C8. *Amino Acids* 2011;40:1195–204.
- [23] Singh R, Ting JG, Pan Y, Teh LK, Ismail R, Ong CE. Functional role of Ile264 in CYP2C8: mutations affect haem incorporation and catalytic activity. *Drug Metab Pharmacokinet* 2008;23:165–74.
- [24] Hichiya H, Tanaka-Kagawa T, Soyama A, Jinno H, Koyano S, Katori N, et al. Functional characterization of five novel CYP2C8 variants, G171S, R186X, R186G, K247R, and K383N, found in a Japanese population. *Drug Metab Dispos* 2005;33:630–6.
- [25] Hanioka N, Matsumoto K, Saito Y, Narimatsu S. Influence of CYP2C8\*13 and CYP2C8\*14 alleles on amiodarone N-deethylation. *Basic Clin Pharmacol Toxicol* 2011;108:359–62.
- [26] Hanioka N, Matsumoto K, Saito Y, Narimatsu S. Functional characterization of CYP2C8.13 and CYP2C8.14: catalytic activities toward paclitaxel. *Basic Clin Pharmacol Toxicol* 2010;107:565–9.
- [27] Soyama A, Hanioka N, Saito Y, Murayama N, Ando M, Ozawa S, et al. Amiodarone N-deethylation by CYP2C8 and its variants, CYP2C8\*3 and CYP2C8 P404A. *Pharmacol Toxicol* 2002;91:174–8.
- [28] Ishikawa C, Ozaki H, Nakajima T, Ishii T, Kanai S, Anjo S, et al. A frameshift variant of CYP2C8 was identified in a patient who suffered from rhabdomyolysis after administration of cerivastatin. *J Hum Genet* 2004;49:582–5.

- [29] Dravid PV, Frye RF. Determination of N-desethylamodiaquine by hydrophilic interaction liquid chromatography with tandem mass spectrometry: application to in vitro drug metabolism studies. *J Chromatogr B Anal Technol Biomed Life Sci* 2008;863:129–34.
- [30] Schoch GA, Yano JK, Wester MR, Griffin KJ, Stout CD, Johnson EF. Structure of human microsomal cytochrome P450 2C8. Evidence for a peripheral fatty acid binding site. *J Biol Chem* 2004;279:9497–503.
- [31] Aquilante CL, Wempe MF, Spencer SH, Kosmiski LA, Predhomme JA, Sidhom MS. Influence of CYP2C8\*2 on the pharmacokinetics of pioglitazone in Healthy African-American Volunteers. *Pharmacotherapy* 2013;33:1000–7.
- [32] Yeo CW, Lee SJ, Lee SS, Bae SK, Kim EY, Shon JH, et al. Discovery of a novel allelic variant of CYP2C8, CYP2C8\*11, in Asian populations and its clinical effect on the rosiglitazone disposition in vivo. *Drug Metab Dispos* 2011;39:711–6.
- [33] Afzelius L, Raubacher F, Karlen A, Jorgensen FS, Andersson TB, Masimirembwa CM, et al. Structural analysis of CYP2C9 and CYP2C5 and an evaluation of commonly used molecular modeling techniques. *Drug Metab Dispos* 2004;32:1218–29.
- [34] Lewis DF. Homology modelling of human CYP2 family enzymes based on the CYP2C5 crystal structure. *Xenobiotica* 2002;32:305–23.
- [35] Ohtsuki S, Schaefer O, Kawakami H, Inoue T, Liehner S, Saito A, et al. Simultaneous absolute protein quantification of transporters, cytochromes P450, and UDP-glucuronosyltransferases as a novel approach for the characterization of individual human liver: comparison with mRNA levels and activities. *Drug Metab Dispos* 2012;40:83–92.